Author/s:
Wesemann, L;Rickett, J;Davis, TJ;Roberts, A

Title:
Real-Time Phase Imaging with an Asymmetric Transfer Function Metasurface

Date:
2022-05-18

Citation:
Wesemann, L., Rickett, J., Davis, T. J. & Roberts, A. (2022). Real-Time Phase Imaging with an Asymmetric Transfer Function Metasurface. ACS Photonics, 9 (5), pp.1803-1807. https://doi.org/10.1021/acsphotonics.2c00346.

Persistent Link:
https://hdl.handle.net/11343/313017

Supporting Information for 'Real-time phase imaging with an asymmetric transfer function metasurface'

Lukas Wesemann,[*,†] Jon Rickett,[‡] Timothy J. Davis,[†] and Ann Roberts[†]

†*ARC Centre of Excellence for Transformative Meta-Optical Systems, School of Physics, University of Melbourne, Parkville 3010, Victoria, Australia*

‡*School of Physics, University of Melbourne, Parkville 3010, Victoria, Australia*

E-mail: Lukas.Wesemann@unimelb.edu.au

Document Information

8 pages, 5 figures, no tables

SI1. Spatial frequency filtering

Visualization of optical phase through spatial frequency filtering

Filtering of the spatial frequency content of an optical field permits the visualization of the phase of a wavefield. To illustrate this we consider a scalar, monochromatic, spatially coherent wavefield with a pure phase-modulation $E(t, x, y, z = 0) = E_0 e^{i\phi(x,y)} e^{-\omega t}$. Here $\phi(x, y)$ describes the phase variation in the $z = 0$ plane, E_0 is a constant and ω is the angular frequency of the wave. The first spatial derivative of a wavefield can be computed through filtering of its Fourier content with a linear optical transfer function (OTF). The relationship between the input- and the output fields for a linear space-invariant optical system is given by $\tilde{E}_{\text{out}}(k_x, k_y) = \mathcal{H}(k_x, k_y)\tilde{E}_{\text{in}}(k_x, k_y)$, where $\tilde{E}_{\text{in}}$ and $\tilde{E}_{\text{out}}$ describe the spatial Fourier transforms of the input and output fields respectively and $\mathcal{H}$ the OTF of the system.[1] For a transfer function $\mathcal{H}(k_x, k_y) \propto k_x$, we then obtain a processed field $E_{\text{out}} \propto \partial E_{\text{in}}/\partial x$. When considering vector effects, the transfer function is replaced by a rank-2 tensor. For a nonlinear dependence of the transfer function on spatial frequency, which corresponds to higher order derivatives, a more complex relationship between phase modulation and resulting intensity is found. Although this permits a degree of visualization of the phase, it can result in artifacts in processed images.[2]

Of particular interest in phase imaging is it to obtain intensity images that allow to differentiate between positive and negative phase gradients. This is achieved for example by differential interference contrast microscopy (DIC),[3] which produces typical pseudo 3D intensity images. In order to achieve this, an additional constant offset around which the optical transfer function is linear, is required. The spin-orbit coupling metasurface under consideration exhibits a near-linear magnitude transfer function around the origin with a constant offset making it suitable to produce pseudo 3D intensity images from incident phase images. Below we provide details on the optical transfer function of the metasurface.

Spatial frequency filtering with spin-orbit coupling metasurface

The simulated transmission spectrum of the metasurface is shown in Fig. S1. The simulation was based on a finite element method (FEM), as described in the Methods section, with input values obtained from the SEM images of the device. The average rod dimensions were $l = (100 \pm 10)$nm and $w = (64 \pm 9)$nm, with grating periodicity in the $x-$ and $y-$directions $P_x = 420\,\text{nm}$, $P_y = 210\,\text{nm}$ and the rod spacing $\Delta y = \Delta x = P_x/4 = 105\,\text{nm}$. The optical constants for Ag and Si_3N_4 used in these calculations are obtained from ref.[4] and ref.[5] respectively. The superstrate and substrate of the metasurface are modelled using a homogeneous refractive index of 1.5. In this configuration the metasurface exhibits three spectral features, with central wavelengths of $\lambda_1 = 685\,\text{nm}$, $\lambda_2 = 724\,\text{nm}$ and $\lambda_3 = 824\,\text{nm}$, that suppress transmission at normal incidence for circularly polarized (CP) light. These reproduce the features in the measured transmission spectrum of the metasurface. We attribute the differences between experiment and simulation wavelengths to deviations between the actual and textbook values of electric permittivity, the precise details of the geometry of the fabricated Si_3N_4 layer and Ag nanorods, and fabrication inaccuracies arising from the electron beam lithography process. If we examine the fields at the feature designated '2' at 724 nm

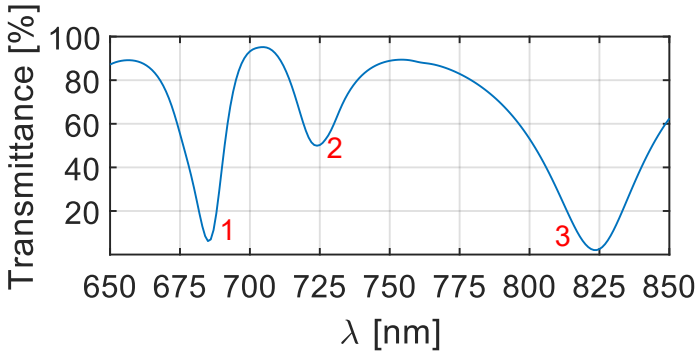

Figure S1: Calculated transmission spectrum of spin-orbit metasurface for normally incident, circularly polarized light.

in Fig. S1 we can see that these correspond to excitation of the waveguiding layer. Fig.

S2a shows the vertical component of the electric field produced in and around the structure when illuminated with normally incident RCP light. The time-averaged Poynting vector at a point in the center of the waveguide in each unit cell shown as a white arrow. The direction of the wave clearly reverses when the devices is illuminated with LCP Fig. S2b. This is further illustrated by the provided supplementary video files that show the propagation of the z-component of the electric field inside of the waveguide for RCP and LCP illumination at $\lambda = 724\,\mathrm{nm}$.

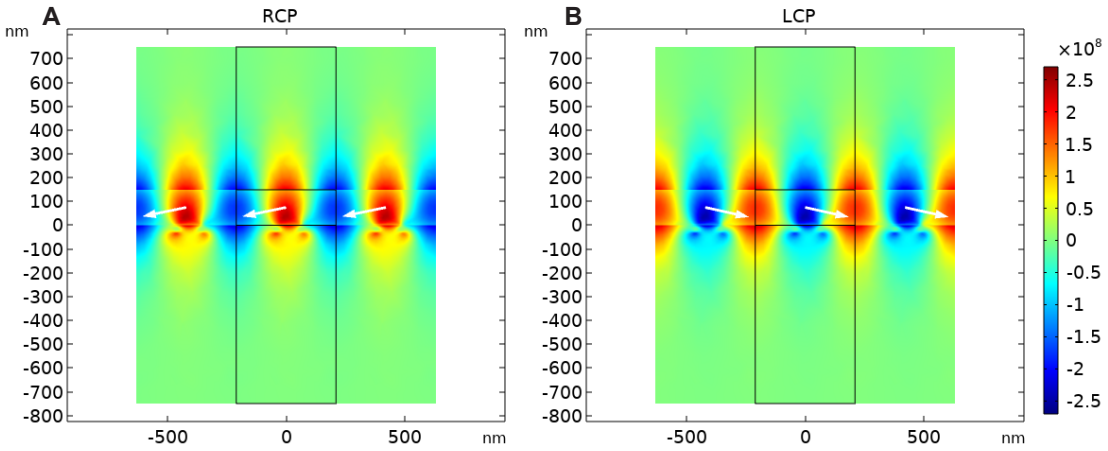

Figure S2: Calculated z-component of the electric field (normalized to the incident field for unit power excitation) for (a) RCP and (b) LCP illumination in the $x-z$ plane. The time-averaged Poynting vector is shown as a white arrow. Normally incident illumination from below.

The metasurface enables asymmetric spatial frequency filtering in transmission using circularly polarized light for operation at the wavelengths where transmission is suppressed. This capacity is characterized by numerically calculating the optical transfer function $\mathcal{H}(k_x, k_y)$ of the device. In figure S3 the magnitude transfer function $|\mathcal{H}(k_x/k_0, ky/k_0)|$ (a,b) as well as the phase transfer function $\arg\left[\mathcal{H}(k_x/k_0, k_y/k_0)\right]$ (c,d) are shown. It is apparent that the device essentially performs a one-dimensional filtering operation along the k_x direction with minor dependence on k_y. In addition to this, the metasurface imposes a negligible phase-shift onto the transmitted field within the interval $[-0.025 < k_x/k_0 < 0.025]$ over which the

metasurface exhibits a near-linear magnitude transfer function.

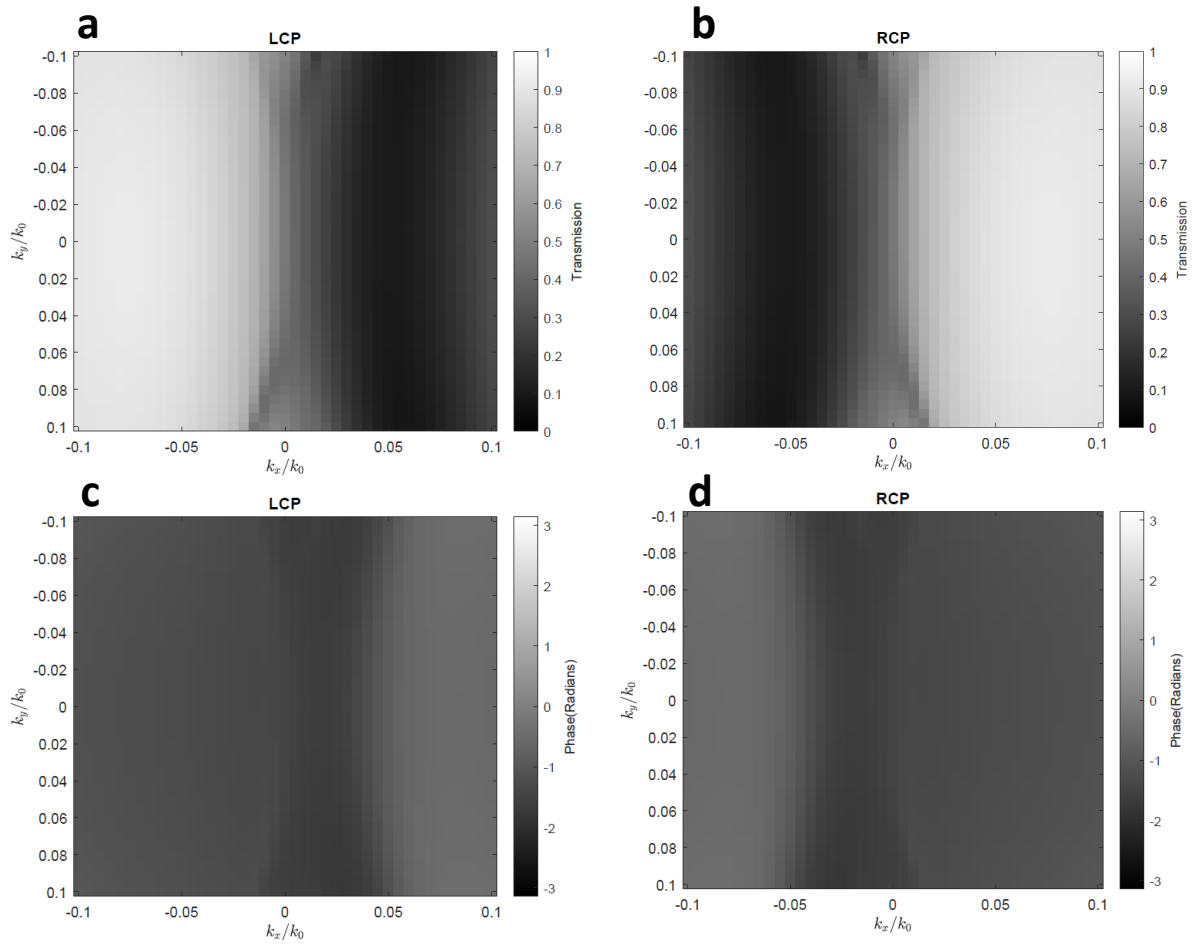

Figure S3: Magnitude transfer function $|\mathcal{H}(k_x/k_0, ky/k_0)|$ (a,b) and phase transfer function $\arg\left[\mathcal{H}(k_x/k_0, k_y/k_0)\right]$ (c,d) of metasurface for RCP (first column) and LCP (second column) incident light.

SI2. Optical Configuration for spectral measurements

The optical configuration for the experimental spectral characterization of the metasurface is shown in Fig. S4. The setup was established on a Nikon Ti-80i inverted microscope using a tungsten halogen light source (Ocean Optics HL-2000 HP). Unpolarized light from the source collimated using a Nikon U PLAN 4x NA0.13 objective (MO1). The collimated beam is subsequently passed through a linear polarizer (Thorlabs LPVIS100) and a quarter-wave

plate (Thorlabs AQWP05M-600) mounted on a rotation stage. This enabled adjusting the angle between the optical axes of the quarter-wave plate and the linear polarizer to $\pm 45°$ thereby switching between right- and left circularly polarized input. The entire illumination unit (MO1, LP and QWP) was mounted on an xyz-stage with integrated rotation module to enable positioning of the input beam adjustment of the incident angle θ_{inc} of the collimated beam onto the metasurface. The metasurface is placed on the integrated stage of the Nikon Ti-80i microscope. The transmitted light is collected by a Nikon LU PLAN LWD 50X 0.5NA

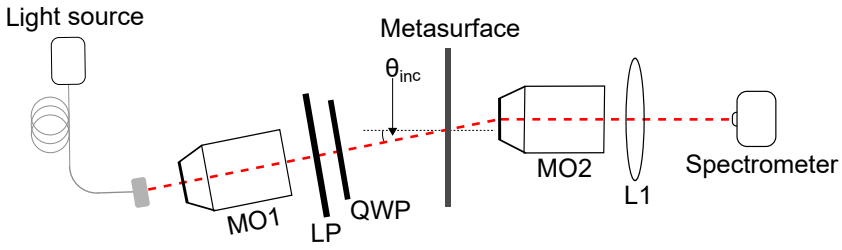

Figure S4: Experimental setup used for the measurement of angle depended spectral transmission characteristics. Light from a tungsten halogen lamp is collimated and circularly polarized before it is transmitted through the metasurface at an adjustable angle of θ_{inc}. The transmitted light is guided to and analyzed by a spectrometer.

objective (MO2). The light is then guided through the the microscope via the microscope's tube lens and subsequently fed into a single mode fiber (Thorlabs SM600) and guided to a spectrometer (Ocean Optics HR2000 + ES High-resolution spectrometer) where the spectral transmission data is recorded. The total area of the metasurface under investigation was $250 \times 250\,\mu\text{m}^2$. The obtained spectra correspond to an averaged result obtained over approximately 80% of the metasurface area due to the field of view of the collecting microscope objective.

SI3. Optical Configuration for SLM Experiments

The phase-imaging experiments in this publication were carried out using the setup shown in Fig. S5 that incorporates a spatial light modulator (Holoeye Pluto 2 VIS014) for the gen-

eration of phase-images. The spatial light modulator (SLM) consists of a 1920×1080 pixel liquid crystal on silicon display with pixel size of $8\,\mu$m. Collimated light from a fiber coupled laser system (NKT Photonics SuperK Compact) with fiber-coupled tunable filter (NKT-Photonics SuperK Select Tunable Multi-line Filter) with a bandwidth of 3 nm (FWHM) is linearly polarised along the operational direction of the SLM. The light reflected from the SLM is passed through a quarter-wave plate (Thorlabs AQWP05M-600) and subsequently demagnified through a telescope consisting of a $f = 150$ mm lens (Thorlabs-LA1433-A) (L1) and a micropscope objective (Nikon UPlanFl 20x 0.5NA) (MO2). The phase-image is pro-

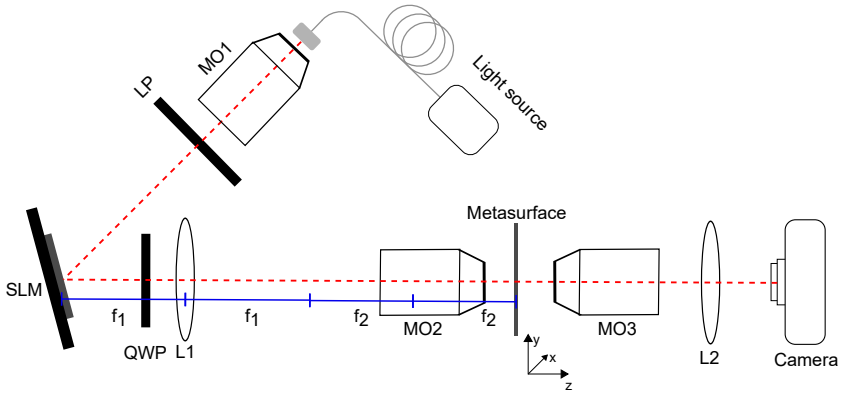

Figure S5: Experimental setup used for the demonstration of phase-imaging via metasurface spin-orbit coupling. Phase-modulations are superimposed onto the wavefield using a spatial light modulation (SLM). The wavefield is circularly polarized, demagnified through a telescope system (L1,MO2) and projected onto the metasurface. The intensity converted image is recorded by a camera.

jected onto the metasurface, which is mounted on an xyz-stage for precise adjustment. The transmitted image is subsequently captured using a microscope objective (Nikon LU Plan 50x 0.55NA) (MO3), and projected onto a camera (Thorlabs DCC1545M) through a $f = 50$ mm lens (Thorlabs LA1131-A) (L2).

References

(1) Goodman, J. *Introduction to Fourier Optics*, 3rd ed.; Roberts and Company, 2005.

(2) Cordaro, A.; Kwon, H.; Sounas, D.; Koenderink, A.; Alù, A.; Polman, A. High-Index Dielectric Metasurfaces Performing Mathematical Operations. *Nano Lett.* **2019**, *19*, 8418–8423.

(3) Lang, W. *Nomarski differential interference-contrast microscopy*; Carl Zeiss, 1982.

(4) Johnson, P.; Christy, R. Optical Constants of Noble Metals. *Phys. Rev. B* **1972**, *6*, 4370–4379.

(5) Luke, K.; Okawachi, Y.; Lamont, M. R.; Gaeta, A. L.; Lipson, M. Broadband mid-infrared frequency comb generation in a Si_3N_4 microresonator. *Optics letters* **2015**, *40*, 4823–4826.